Gluing for Raman lidar systems using the lamp mapping technique

Monique Walker,[1,*] Demetrius Venable,[2] and David N. Whiteman[3]

[1]NASA Post-Doctoral Fellow/ORAU, NASA Goddard Space Flight Center, Greenbelt, Maryland 20771, USA

[2]Department of Physics and Astronomy, Howard University, Washington DC 20059, USA

[3]NASA Goddard Space Flight Center, Greenbelt, Maryland 20771, USA

*Corresponding author: Monique.N.Walker@nasa.gov

Received 22 July 2014; revised 17 November 2014; accepted 18 November 2014; posted 19 November 2014 (Doc. ID 217387); published 19 December 2014

In the context of combined analog and photon counting (PC) data acquisition in a Lidar system, glue coefficients are defined as constants used for converting an analog signal into a virtual PC signal. The coefficients are typically calculated using Lidar profile data taken under clear, nighttime conditions since, in the presence of clouds or high solar background, it is difficult to obtain accurate glue coefficients from Lidar backscattered data. Here we introduce a new method in which we use the lamp mapping technique (LMT) to determine glue coefficients in a manner that does not require atmospheric profiles to be acquired and permits accurate glue coefficients to be calculated when adequate Lidar profile data are not available. The LMT involves scanning a halogen lamp over the aperture of a Lidar receiver telescope such that the optical efficiency of the entire detection system is characterized. The studies shown here involve two Raman lidar systems; the first from Howard University and the second from NASA/Goddard Space Flight Center. The glue coefficients determined using the LMT and the Lidar backscattered method agreed within 1.2% for the water vapor channel and within 2.5% for the nitrogen channel for both Lidar systems. We believe this to be the first instance of the use of laboratory techniques for determining the glue coefficients for Lidar data analysis. © 2014 Optical Society of America

OCIS codes: (040.5250) Photomultipliers; (010.3640) Lidar; (010.7340) Water; (120.0280) Remote sensing and sensors; (280.3640) Lidar; (290.5860) Scattering, Raman.

http://dx.doi.org/10.1364/AO.53.008535

1. Introduction

The lamp mapping technique (LMT) has recently been demonstrated as a means of independently calibrating the Raman lidar water vapor mixing ratio (WVMR) [1]. In particular, Venable *et al.* showed that the WVMR calibration value determined using the LMT agreed to within 5% of the value obtained through the more traditional technique that derives the Lidar calibration by comparison with radiosondes. In this paper we will focus on a new application of the LMT, that of determining glue coefficients used in the analysis of Lidar data. Gluing is the term that is used for the technique of combining simultaneously acquired analog-to-digital (AD) and photon counting (PC) Lidar data into a single profile [2,3]. The technique that is usually performed involves a linear regression of the analog and PC ordered pairs. The slope and intercept obtained from the regression are the "glue coefficients." Where the PC count rate is greater than 10 MHz, we use the glue coefficients to convert the analog signal to a virtual PC signal. However, in the presence of clouds, it can be problematic to calculate glue coefficients using atmospheric profile data because clouds attenuate the signal and the resulting fast transients may not be tracked equally well by both AD and PC technologies. It is also difficult, and in some cases impossible, to obtain accurate Lidar glue coefficients in the daytime due to high

1559-128X/14/368535-09$15.00/0
© 2014 Optical Society of America

Table 1. Two Lidar Systems Details

	HURL	ALVICE
Laser emission	355 nm	355 nm
Power	8–10 W	10–16 W
Measured light	Aerosol 355 nm, Water Vapor 408 nm, Nitrogen 387 nm	Aerosol 355 nm, Water Vapor 408 nm, Nitrogen 387 nm
Laser rep. rate	30 Hz	50 Hz
Light coupling	Fiber Coupled	Direct Coupled
Telescope diameter	400 mm	600 mm
Interference filter width analog	Nitrogen filter 0.30 nm, Water Vapor filter 0.24 nm	Nitrogen filter 0.19 nm, Water Vapor filter 0.27 nm
Sampling range	Water Vapor ch. 0–20 mV, Nitrogen ch. 0–100 mV	Water Vapor ch. 0–20 mV, Nitrogen ch. 0–20 mV

solar background [3]. Previous efforts have determined that the preferred way to deal with this difficulty is to use nighttime Lidar data to determine glue coefficients that are then used for processing both nighttime and daytime data [2,3]. For example, Newsom *et al.* [3], achieved much better agreement between integrated precipitable water measurements from the Lidar and microwave radiometer when using this approach versus attempting to determine glue coefficients in the presence of high solar background.

2. Method

A. Description of Raman Lidars

In this paper, we make use of the LMT [1] to calculate glue coefficients for Lidar data acquisition systems where the measurements are made by scanning a halogen lamp over the Lidar receiver telescope, a procedure that is done completely within the laboratory environment, thus eliminating the possibility of atmospheric influences and interference of the solar background. We compared glue coefficients determined from atmospheric profiles acquired by the usual method, which we call the Lidar backscatter method (LBM) as discussed in Whiteman *et al.* [2] and Newsom *et al.* [3], to glue coefficients determined from the LMT that we will discuss here. We consider the glue coefficients derived using the LBM to generally be the reference values for comparison purposes although there are occasions, that we will clarify later, where the glue coefficients derived using the LMT may be preferred.

This study was conducted on two Raman lidar systems. The first system was the Howard University Raman Lidar (HURL) system [4,5]. This system utilizes the third harmonic output of a Nd:YAG laser as the emitter and measures Rayleigh/Mie signals at 355 nm and Raman-shifted nitrogen and water vapor signals at 387 nm and 408 nm, respectively (Table 1). The HURL system uses Licel transient recorders [6] for data acquisition. For the experiments performed here, 16,000 bins of data were acquired in each profile, where each bin corresponded to a spatial resolution of 7.5 m. The other Raman lidar system involved in this study was the NASA Atmospheric Laboratory for Validation Interagency Collaboration and Education (ALVICE) system [7–9]. ALVICE also uses the third harmonic output of a Nd:YAG laser (355 nm) and measures the same signals mentioned above as in HURL (Table 1) as well as aerosol depolarization, liquid/ice water scattering, and two pure rotational Raman signals for determining atmospheric temperature [7–9]. The ALVICE system also uses Licel transient recorders for data acquisition. These Licel transient recorders (Table 2) simultaneously sample the Lidar profile using both analog and PC data acquisition electronics creating the raw signals that need to be combined through the gluing process.

A combination of analog and PC electronics has been found to greatly extend the capabilities of a nonsolar blind Raman lidar, operating in an upward looking configuration, to measure the WVMR throughout the diurnal cycle [2]. Analog measurements are typically preferred in the near field or where signals are high. PC is generally preferred in the far field or where signals are low. For these experiments, the HURL data were acquired every minute at a laser repetition frequency of 30 Hz, while for ALVICE, data were acquired every two minutes at a repetition rate of 50 Hz.

In the LBM as implemented here, the glue coefficients (slope and intercept) are determined for each profile of 16,000 bins by taking the linear regression of the order pairs formed from the background corrected AD voltage levels and the response-time-corrected [2,10,11] PC data. We note here first that there is a propagation delay difference between the analog and PC circuitry that must be accounted

Table 2. Licel Transient Recorders

Licel Specifications	
Model number	TR 20-160
AD resolution	12 Bit
Sampling rate	20 MHz
PC Max count rate	250 MHz
Least significant bit at 20 mV	4.88×10^{-6} V
Least significant bit at 50 mV	12.2×10^{-6} V
Least significant bit at 100 mV	24.4×10^{-6} V
Number of bins	16,000

for prior to forming the ordered pairs. In practice, we account for this delay by offsetting the bin numbers between the AD and PC signals using values provided by the manufacturer that are easily verified using actual measurements. For HURL, there is a difference of 3 bins between the AD and PC signals, and for ALVICE the difference is 7 bins due to the different versions of the Licel transient recorders in use. Also, we use a simple nonparalyzable assumption to correct the PC data since this model avoids the convergence issues of more complicated assumptions [12,13] and the maximum count rate of the data prior to correction is 10 MHz, for which the uncertainty in the correction is much less than 1% [9]. The glue coefficients are individually determined for each profile, then the average of all the individual profile glue coefficients is determined and these average values are used as the final set of glue coefficients. The final glue coefficients (average slope, average intercept) are used to create a function that is used to convert the AD voltage signal into an equivalent signal in PC rate space (Hz).

To clarify what is being done in this paper for the purposes of calculating the WVMR from Raman Lidar data, we do not first form the ratio of the water vapor and nitrogen PC and analog signals and then attempt to combine these signals in some manner to create the final profile. Instead, we are gluing the AD and PC signals of the water vapor and nitrogen channels separately. This is the preferred way to do it since, due to the large differences in signal strengths of the backscattered Lidar data, there is a significant difference in the optimum gluing altitude ranges for the water vapor and nitrogen signals [3]. In addition, the gluing procedure described here permits the resolving time value that is needed to correct PC data to be optimized by studying the intercepts of the regressions [2]. (We note later, however, that for the study done here the resolving time used was determined using an earlier study based on LBM results.) Therefore we glue each channel separately and then take the ratio of the two signals to create a single profile, as done by Whiteman *et al.* and Newsom *et al.* [2,3].

In the lamp mapping experiment, which we routinely do before every data acquisition session, the halogen lamp is scanned over the entire telescope to provide a range of count rates as a function of position on the telescope [1]. For example, when the lamp is close to the optical axis the count rates are generally higher than at the edge of the telescope. This variability in count rate as a function of position enables a regression of ordered pairs to be performed to determine glue coefficients. Therefore, the study discussed here could not be done with a constant intensity lamp in a fixed position because no change in the signal intensity would be expected.

B. Lidar Backscatter Glue Technique

Here we discuss the technique for determining glue coefficients using the LBM [2,3], which entails using actual atmospheric profiles as the source of data to perform the gluing. We consider this to be the reference method for determining glue coefficients since it is the one that is available in all Lidar systems with dual AD and PC data acquisition systems. As mentioned previously, glue coefficients are found by performing a linear regression of simultaneously acquired analog and PC data for an individual channel.

To convert the analog signal into units of volts we use the following:

$$AD_i = \frac{A_i V_s}{(2^{12} - 1)\, s}\ , \tag{1}$$

where A_i are the raw analog data (counts) per bin for the ith bin, V_s is the voltage scaling factor for the recorder, s is the number of shots, and $2^{12} - 1$ accounts for the number of digitization levels of a 12 bit AD converter. The background is then subtracted from the analog signal. The background is defined here as the signal due to the absence of light. Therefore, we block any light from getting into the detectors by closing the shutters to obtain a background signal. In practice, we take the average background signal determined over 5–10 min to subtract from the analog signal. We also convert the PC signal to count rates (Hz), C_i.

$$C_i = \frac{PC_i}{T}, \tag{2}$$

where PC_i are the PC data (counts) per bin for the ith bin and T is the time required to accumulate the counts. Upon obtaining photon count rates, we correct the photon count rate for the response time. Generally, the response time correction is larger for higher count rates and accounts for photons that may not have been counted properly due to bandwidth limitations [2,11]. Our experience is that these resolving times are a function of the specific PMT and PC hardware being used and can be considered constant in the absence of hardware degradation. For that reason, the resolving times used in the processing of the LMT data done here have been determined using previously performed LBM measurements. The correction for this response time nonlinearity that we use can be expressed as

$$C_i' = \frac{C_i}{1 - \tau_r C_i}, \tag{3}$$

where C_i are the uncorrected count rates and τ_r is the response time [2,5,10,11]. Equations (1)–(3) are described in detail in Newsom *et al.* for the LBM [3], but we reintroduce them here to make comparisons to the new equations for the LMT that will be shown later [Eqs. (5)–(7)].

When converting the AD data to a virtual PC scale, and then gluing the data sets, we first perform a linear regression of the corrected (PC, AD) ordered

pairs. For the LBM the corrected ordered pairs are (C'_i, AD_i). When taking the linear regression of the ordered pairs the appropriate units for the PC data is Hz and for the AD data is volts. The glue coefficients (slope and intercept), determined from the regression just mentioned, are used to convert the AD signal into a PC signal by using the equation

$$C = m'D + b', \tag{4}$$

where C is the virtual photon count rates, D is the corrected analog signal, $m'(1/m)$ is the slope, and $b'(-b/m)$ is the intercept [3]. Note the switching of the independent and dependent variable for the linear regression of the order pairs in Eq. (4). This is done to compensate for the asymmetrical way that data are selected when using count rate cutoff values and is described in detail by Newsom *et al.* [3]. In this paper we discuss the two parameter regression to determine glue coefficients as used by Newsom *et al.* [3] and Whiteman *et al.* [2]. This method is discussed in detail in Newsom *et al.* We now apply the Newsom method to the Lidar backscattered data and to the lamp mapping data to find the glue coefficients.

C. Lamp Map Technique for Determining Glue Coefficients

Here we discuss how to find the glue coefficients using the LMT, which entails using the signal from a scanned halogen lamp as the source of data to perform the gluing. The data acquisition system runs in an identical manner as for acquiring atmospheric profiles. However, in this method, with the lamp positioned at a specific location the signal presented to the detection system is approximately constant and varies randomly around a constant value within each "profile." When using the LMT, variation in the count rate is achieved by moving the lamp to different locations above the telescope where higher or lower count rates are achieved. By contrast, when using the LBM technique the signal count rates vary significantly within each profile. The LMT PC and AD signal corrections are determined slightly differently than when using the LBM technique since the count rate values using the LMT technique vary as a function of lamp position in front of the telescope and not as a function of "range" within a given "profile." For the LMT we use the average PC and AD counts per profile for the PC and AD data and then take the linear regression of the average values for all profiles, whereas in the LBM we take the regression of the ordered pairs of AD and PC data in each individual profile. One "profile" is acquired at each location of the lamp when using the LMT. The lamp is moved to each position and stops at each position and then data are acquired. A significant difference between the LBM and LMT, therefore, is that the LMT gluing uses the counts from the constant halogen light source and the LBM gluing uses the counts from the transient backscattered laser light and for this reason the equations used in this technique [Eqs. (5)–(7), below] must differ in small but significant ways from Eqs. (1)–(3).

The photon count rates for the LMT are a modified version of Eq. (2),

$$C_j = \frac{\sum_{i=1}^{n} PC_{ij}}{Tn}, \tag{5}$$

where PC_{ij} are the photon counts per bin (i) for the jth position of the lamp during the scan. So C_j are the average count rates per jth position. The response time corrected count rates are determined similarly as in Eq. (3),

$$C'_j = \frac{C_j}{(1 - \tau_r C_j)}. \tag{6}$$

We modify Eq. (1) for converting the AD data to volts for the LMT for the reasons described above,

$$D_j = \frac{(\sum_{i=1}^{n} A_{i,j}) V_s}{(2^{12} - 1) sn}, \tag{7}$$

where $A_{i,j}$ are the AD counts per bin (i) for the jth position of the lamp during the scan. D_j is the average AD signal for the jth position per shot and $n = 16,000$ bins. Next we "background correct" D_j (analog signal). We first determine the D_j value that corresponds to the PC value equal to zero. To do this we take the linear regression of the (C'_j, D_j) order pairs and then we use Eq. (4) to solve for the background correction value when $C = 0$ using previously determined resolving time values that have been found to be essentially constants for our systems. Upon determining the D_j at $C = 0$ (D_{zero}), we subtract D_{zero} from all D_j LMT profiles and therefore we obtain the corrected AD signal, D'_j. This "background correction" is important for the analog signal and must be performed carefully due to temporal changes in the acquisition system, a concept that will be discussed later. It should be noted that the background correction method described here for the analog signal is different for the LMT and LBM. The (C'_j, D'_j) are then the corrected signals from the LMT used to determine the glue coefficients (slope and intercept), which will be used in Eq. (4).

3. Results

A. HURL Gluing Results

In this section, we compare glue coefficients determined from the LMT and from the traditional LBM based experiments done with the HURL Lidar system. For the LMT we used a 20 mm step size for the scans and a 5-second accumulation time for each sample. The lamp was scanned across the whole aperture of the HURL telescope, which is 400 mm in diameter. The lamp used was a 200 W calibrated halogen lamp. For the LMT gluing, we eliminated

Table 3. Glue Coefficients for HURL from LBM and Glue Coefficients Determined from LMT

HURL LBM Glue Coefficients		
	Slope (10^{10} Hz/V)	Intercept (10^3 Hz)
Nitrogen channel	9.51 ± 0.03	51 ± 13
Water vapor channel	10.51 ± 0.14	-1 ± 4
HURL LMT Glue Coefficients		
	Slope (10^{10} Hz/V)	Intercept (10^3 Hz)
Nitrogen channel	9.62 ± 0.39	19 ± 94
Water vapor channel	10.59 ± 0.17	13 ± 49

outliers in the data by rejecting points that are more than 1.5 standard deviations from the regression line, which is also done for the LBM [2]. We also regress the data only in the region where we expect linearity between the AD and response-time-corrected PC data, a range taken to be between 1 and 10 MHz, as for the LBM [2,14]. For the LMT technique applied to HURL, we regressed the data between the count rate ranges of 1 and 4 MHz for the water vapor and nitrogen channels.

We compared the glue coefficients obtained using the LMT and LBM techniques for the HURL system. For the LMT, 8 determinations of the glue coefficients were performed during the period of 25 October 2012 to 02 January 2013. For the LBM, 5 determinations were performed between 14 November 2012 and 19 December 2012. Table 3 compares the average glue coefficients and the standard deviations obtained from these two sets of measurements. The LBM count rate range used for the regressions of the nitrogen data was 1–10 MHz, while for the water vapor channel the range was only 0.05–1 MHz due to the low signal intensity in the water vapor channel. While, in general, the LBM-derived glue coefficients are considered the reference under dry conditions, the count rate range provided by the LMT results can exceed that of the LBM-derived results providing a more robust regression. This is the case for the HURL water vapor channel. In such cases, we consider the LMT coefficients to be preferred, although the two results agree quite closely, as shown in Table 3.

The data in Table 3 were acquired over a period of 2–3 months. The slopes found using the LBM and LMT agree within 1% for HURL. The intercepts found using the LBM and LMT do not agree as well but are within 1 standard deviation of each other, and this difference is considered to be statistically insignificant. The intercept value (in units of Hz) is typically orders of magnitude smaller than the determined count rate value, so the variability in the intercept has little influence on the values generated by Eq. (4) when using glue coefficients obtained by either the LBM or LMT.

While it is interesting to compare the glue coefficients of the two methods as done in Table 3, a more direct comparison of the two techniques is achieved by evaluating Eq. (4) and comparing the glued results. Figures 1(a) and 1(b) are plots of Eq. (4) using the average glue coefficients shown in Table 3 versus the ordered pairs from 10 Lidar profiles for the water vapor [Fig. 1(a)] and nitrogen channels [Fig. 1(b)]. In Figs. 1(a) and 1(b), the LMT-determined functions are shown in red, the LBM-determined functions are shown as the black dashed line and the gray dots are the LBM ordered pairs. The R-squared values for the LBM water vapor and nitrogen channel data [gray dots in Figs. 1(a) and 1(b)] are 0.95 and 0.99, respectively. The embedded plots in Figs. 1(a) and 1(b) show the same LMT and LBM glue functions (red line and black line, respectively) as the outer plots, as well as the LMT ordered pairs (black dots). The R-squared values for the LMT water vapor and nitrogen channel data [black dots in embedded plots in Figs. 1(a) and 1(b)] are 0.99 and 0.95, respectively.

We now compare the virtual PC values using the overall average glue coefficients obtained from the 8 LMT cases to the virtual PC values using the overall average glue coefficients obtained from the 5 LBM cases for both the water vapor and nitrogen channels. We should point out that above 10 MHz only converted AD data are used, and below 10 MHz the resolving time corrected PC data are used. Thus, we confine the investigation of the relative differences between the LBM and LMT to virtual PC values above 10 MHz. Figures 1(c) and 1(d) show that the maximum relative difference between the LBM and LMT-determined glued values for the water vapor channel [Fig. 1(c)] is $\sim -1.2\%$ for photon count rates ranging between 10 and 100 MHz. A similar analysis of the nitrogen channel indicates a maximum relative difference of $\sim -0.8\%$ [Fig. 1(d)]. Therefore, for both the water vapor and nitrogen channels, the LMT and LBM glue functions are within ~1% agreement in the high count rate range where the converted AD data are used. As mentioned before we only glue the data above 10 MHz but the LMT and LBM glue functions are in good agreement in the lower count rate range as well as can be seen in Figs. 1(a) and 1(b) for the water vapor and nitrogen channel, respectively.

The relative standard error (standard deviation/mean) of the LBM-determined glue functions, as shown in Figs. 1(a) and 1(b), is 1% for the water vapor channel and less than 1% for the nitrogen channel over a 2 month period. The relative standard error for the LMT, as shown in Figs. 1(a) and 1(b), is 4% for the water vapor channel and 5% for the nitrogen channel over a 4 month period.

B. ALVICE Gluing Results

In this section we perform a similar analysis of the LMT and LBM-determined glue functions as just performed using HURL data but this time using measurements from the Raman lidar in the ALVICE mobile laboratory. We also used a 200 W lamp on ALVICE for the LMT. For these LMT measurements, we used a 33 mm step size for the halogen lamp scans across the aperture of the telescope and a 1-second

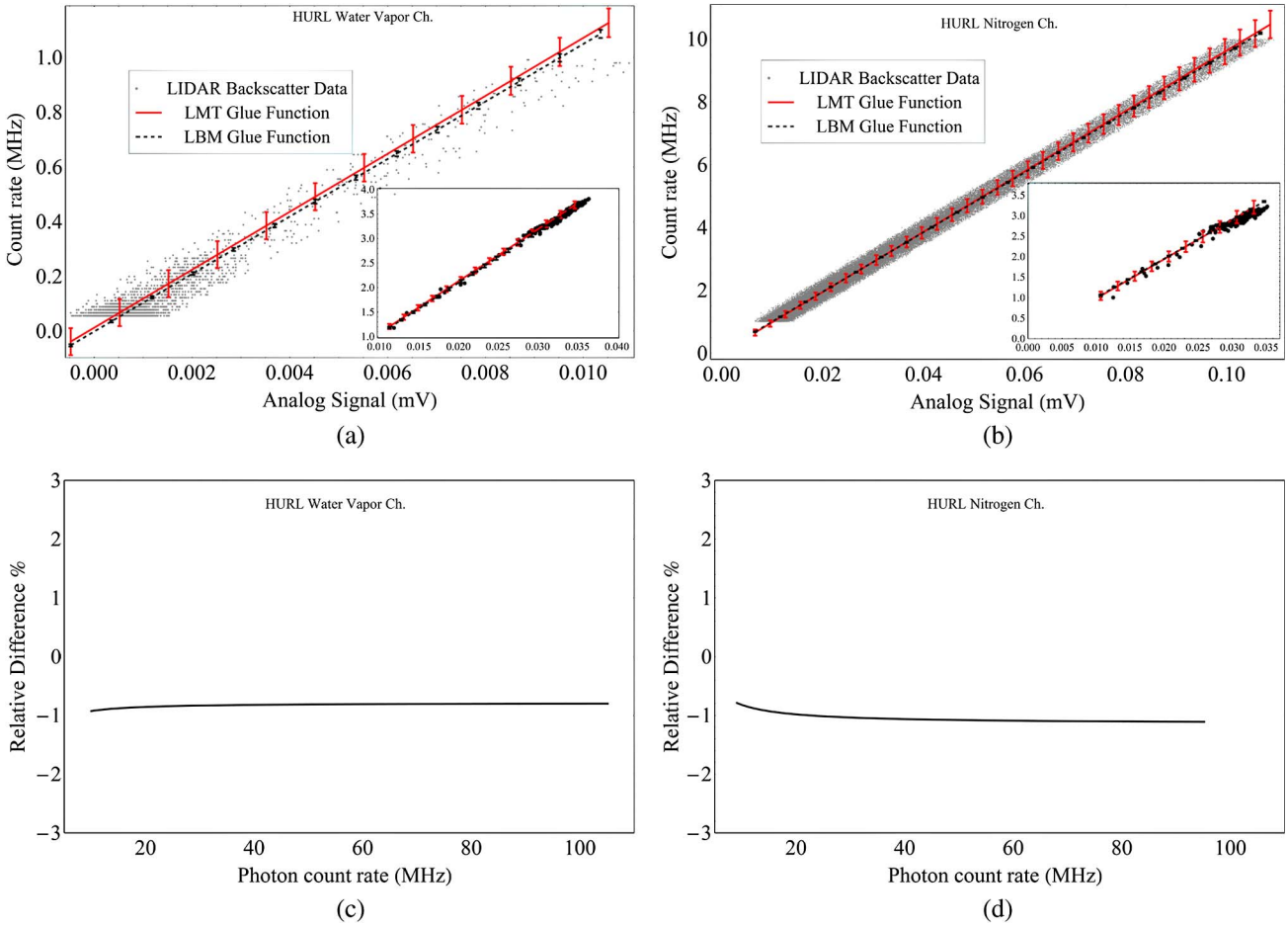

Fig. 1. Comparison between the average LMT glue function (red solid line) and average LBM glue function (black dashed line) for the (a) water vapor (b) and nitrogen channels. The gray dots are the PC and AD ordered pairs from the LBM. The data points are the backscatter data [(a) and (b)]. The imbedded plots show the LMT ordered pairs (black dots) along with the LMT and LBM glue functions. The lower graphs are the HURL relative differences [100 (LBM-LMT)/LBM] between the LMT-determined glue function and LBM-determined glue function for (c) water vapor channel and (d) nitrogen channel.

accumulation time for each point. For ALVICE, the LMT step size was larger and the accumulation time was shorter than for HURL. The larger step size and decreased accumulation time permitted scans to be done across the 600 mm telescope of the ALVICE system in ~15 min. We used the average of three lamp mapping scans to determine glue coefficients for the water vapor channel and the average of two lamp mapping scans to determine the nitrogen channel glue coefficients. The LMT provided PC data from 0.05 to 5.0 MHz for the water vapor channel and 0.05 to 0.8 MHz for the nitrogen channel. The ALVICE glue coefficients determined from the LBM were obtained from the average of 10 clear nights of actual Lidar measurements, using data within the count-rate range of 1–10 MHz for both the nitrogen and water vapor channels. As opposed to the result in the HURL-based experiments, the count rate range achieved in the ALVICE measurements were larger for the LBM measurements than the LMT ones. For this reason, although the results using the two techniques shown in Table 4 agree within 1 standard deviation, we consider the LBM results to likely be more accurate.

As before, we wish to compare the values determined from the glue functions using the glue coefficients determined from the LMT and LBM [Figs. 2(a) and 2(b)] experiments. Here we are comparing Eq. (4) using the overall average glue coefficients determined from the LMT experiments (red solid line) and the LBM experiments (black dashed line). These functions are plotted against ordered pairs of (AD, PC) data from 10 profiles of the water vapor and nitrogen channels [Figs. 2(a) and 2(b) gray dots]

Table 4. ALVICE Glue Coefficients from LBM and LMT[a]

HURL LBM Glue Coefficients		
	Slope (10^{10} Hz/V)	Intercept (10^3 Hz)
Nitrogen channel	9.51 ± 0.03	51 ± 13
Water vapor channel	10.51 ± 0.14	-1 ± 4
HURL LMT Glue Coefficients		
	Slope (10^{10} Hz/V)	Intercept (10^3 Hz)
Nitrogen channel	9.62 ± 0.39	19 ± 94
Water vapor channel	10.59 ± 0.17	13 ± 49

[a]Note the ALVICE LMT results shown here were limited to two data sets.

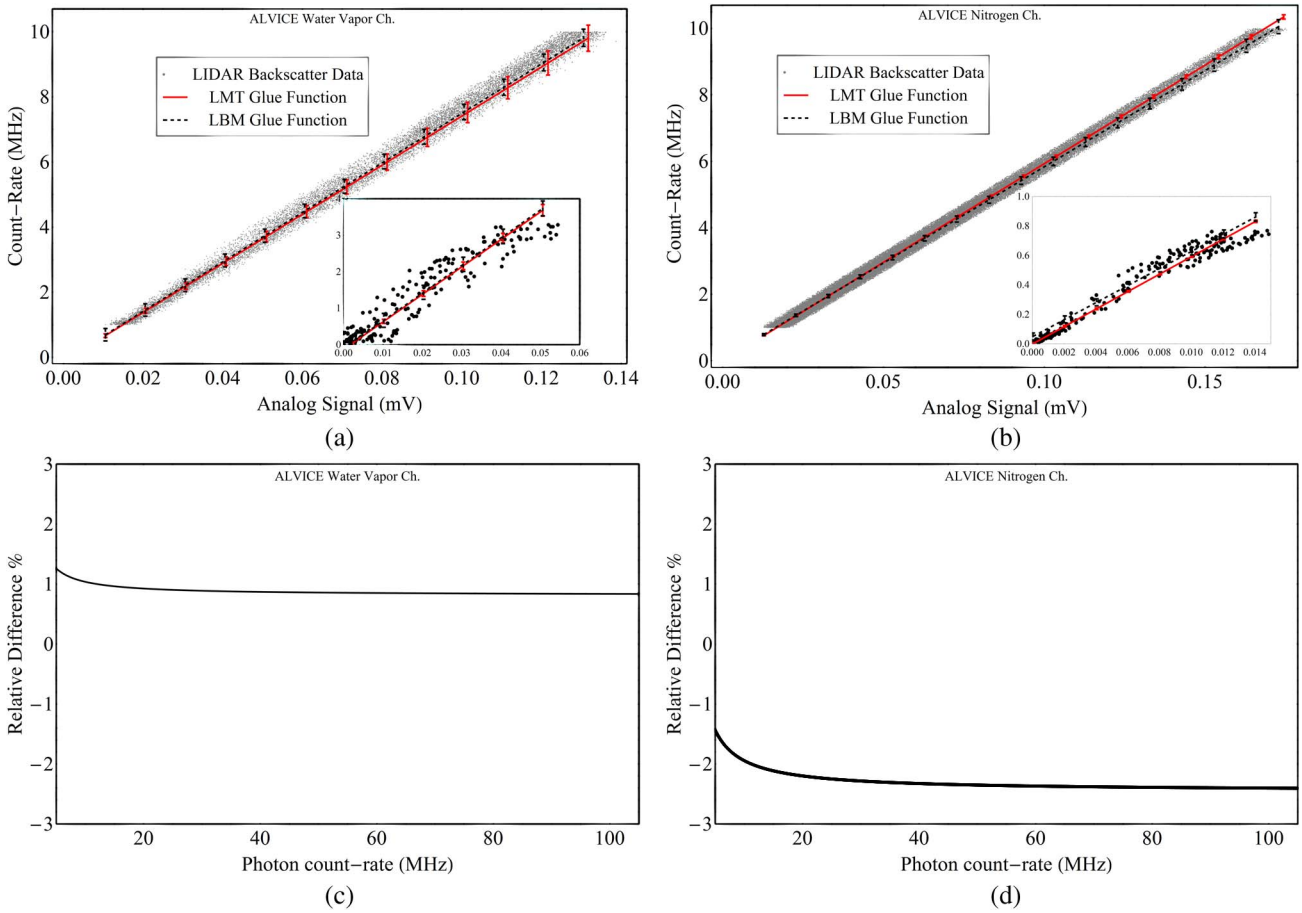

Fig. 2. A plot of average glue functions for LMT (red solid line) and LBM (black dashed line) for ALVICE (a) water vapor and (b) nitrogen channels. The gray dots are the PC and AD ordered pairs from the LBM. The embedded plots show the LMT ordered pairs (black dots) along with the LMT and LBM glue functions. The two lower plots are the relative differences [100 (LBM-LMT)/LBM] for the ALVICE LMT-determined glue function and LBM-determined glue function for (c) the water vapor channel and (d) the nitrogen channel.

for ALVICE. The R-squared values for the LBM water vapor and nitrogen channel data [gray dots in Figs. 2(a) and 2(b)] are both 0.99. The embedded plots in Figs. 2(a) and 2(b) show the same LMT and LBM glue functions (red line and black dashed line, respectively) as the outer plots, as well as the LMT ordered pairs (black dots). The R-squared values for the LMT water vapor and nitrogen channel data [black dots in embedded plots in Figs. 2(a) and 2(b)] are 0.90 and 0.96, respectively.

To further investigate the average LMT glue function versus the LBM glue function we compare the relative differences of the virtual PC values determined from the LMT and LBM glue functions as we did for HURL. Again, the glue function is only applied to Lidar data count rates above 10 MHz; therefore, we focus on the performance of the glue functions above 10 MHz. As can be seen in Figs. 2(c) and 2(d), the LMT and LBM virtual PC values have a maximum relative difference of ~1.2% for the water vapor channel for the photon count rate range of 10–100 MHz and the nitrogen channel determined glue functions have maximum relative differences of $\sim -2.5\%$ for a photon count rate range of 10–100 MHz. The larger differences for the ALVICE nitrogen channel compared to the HURL experiments could be attributed to the relatively low count rates in the narrow nitrogen spectral channel and the small number of experiments (2) performed using the LMT.

C. LBM versus LMT Water Vapor Mixing Ratio

In this section we discuss how the WVMR profile calculated from the LMT-determined glue function compares with the WVMR profile calculated from the LBM-determined glue function. We applied the average glue coefficients found in Table 3 for the LBM and LMT to one night of HURL data. After calibration, we compared the WVMR profiles determined using both the LMT- and LBM-determined glue functions. As expected, Fig. 3 shows that the two WVMR profiles agree to within ~1%.

D. Transient Recorder Warm Up

Throughout this study we have found that the Licel transient recorders require a period of time to warm up and for their performance to stabilize. Specifically, the user settable DC voltage offset that pertains to the analog part of the system showed a steady increase in value as a function of time (Fig. 4) for about

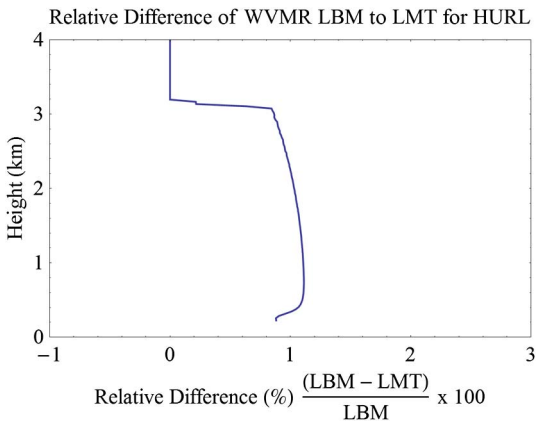

Fig. 3. Plot of the WVMR relative differences using the LBM glue function versus the LMT glue function. This plot shows a maximum relative difference of ~1% between the WVMR determined using the LBM and LMT techniques.

60 min after the initial turn-on. Therefore, it is important to allow the Licel transient recorders to warm up for at least 60 min before taking data for the LMT experiment. If the transient recorders are not thermally stabilized, it will affect the determination of the LMT glue coefficients following the procedure outlined here.

In Fig. 4, we plot the AD and PC signals under dark conditions over a period of time. Because we are plotting background we expect the PC signal to be zero and the AD to be a constant DC offset value greater than zero. In Fig. 4 we see a steady rise of the AD signal during the first 30–60 and the signal stabilizes at ~1.22 mV for the nitrogen channel [Fig. 4(a)] and 1.05 mV for the water vapor channel [Fig. 4(b)]. After 60 min we see a slight increase of the AD offset value, but this slight increase beyond 60 min is less than 1 least significant bit from the asymptote. Note that the least significant bit ranges from 4.884×10^{-6} V to 2.442×10^{-5} V for full scale voltage ranges of 0–20 mV and 0–100 mV, respectively, which are the voltage ranges used for the water vapor and nitrogen channel, respectively, for the data shown. Therefore, this warm-up phenomenon can be seen to increase the DC offset in these cases (for HURL) by ~9 bits for the water vapor channel (0–20 mV range) and ~3 bits for the nitrogen channel (0–100 mV range).

4. Discussion and Conclusion

Our research indicates that the LMT technique has benefits to Lidar research beyond the original intention of supporting an independent calibration of a Raman water vapor Lidar [1]. Here we have found that the data acquired by scanning a halogen lamp across the Lidar receiver telescope can be useful for aiding the "gluing" of analog and PC data when using electronics that simultaneously measure both analog and PC signals. Experiments performed on two different Raman lidar systems were discussed. The relative differences between the glued values determined from the LMT and LBM for the water vapor channels of both Lidar systems was ~1.2% or less and for the nitrogen channel 2.5% or less. Therefore, the WVMR data glued using either the LMT or LBM would agree to within ~2% using either set of glue coefficients. We expect that the higher differences reported for the ALVICE nitrogen channel are due to poor count statistics and could be improved with a more intense lamp and a larger number of experiments. Using either the LMT or the LBM, the slopes determined showed lower variability than the intercepts in percentage terms although the variation in offset values was not significant in the determination of the glued values.

It is also important to note that the transient recorders are temperature sensitive. Therefore, the studies conducted here were performed after a warm-up time of at least 30 min. We conclude that it is best to take analog measurements after the transient recorders have thermally stabilized. Depending on how the analysis is performed, the transient recorder warm-up issue may affect results using either the LBM or LMT. However, the LBM employed here measures transient signals where the background is corrected for each profile and thus is less

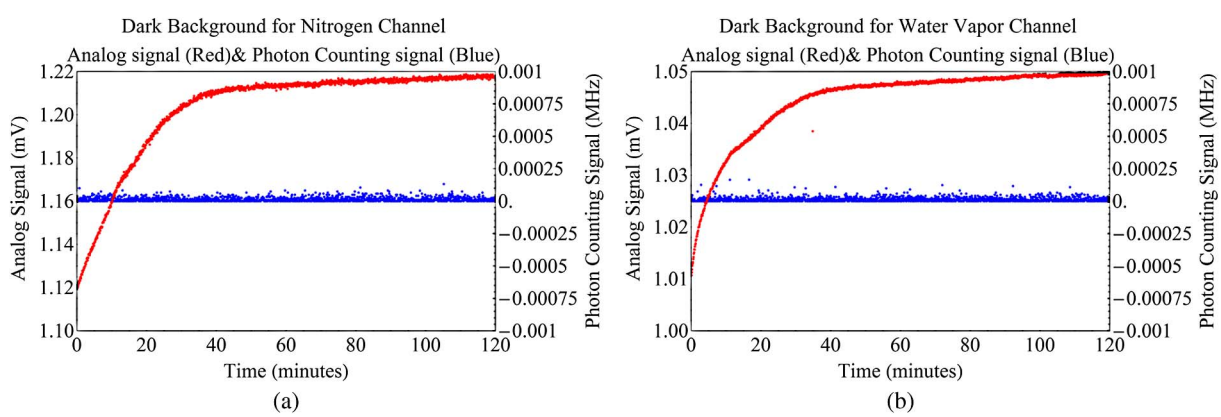

Fig. 4. The values of the DC offset for both (a) the nitrogen and (b) water vapor channels are shown for HURL. The values stabilize after approximately 60 min. The red curved line is the analog signal and the blue flat line is the PC signal. Acquiring data prior to the completion of this warm-up period can result in anomalous gluing results if using a mean gluing value as discussed in the text.

susceptible to the warm-up issues in the transient recorders.

Overall there are a number of advantages offered by using the LMT versus the Lidar backscattered method to obtain glue coefficients. As mentioned before, the LMT can determine glue coefficients without concerns for the amount of solar background or for atmospheric obstructions such as clouds. It also can be done under any weather conditions, as the measurements are completely confined to the laboratory. This means that the glue coefficients are more reflective of the performance of the detectors and transient recorders and not influenced by atmospheric conditions. However, we will note that the LMT's performed here, for the determination of the glue function, had a higher standard deviation than the LBM. Therefore, it is recommended to use the traditional LBM for the determination of the glue coefficients during clear sky conditions and to use the LMT to determine glue coefficients when high solar background or clouds are present. Also, the LMT method for determining glue coefficients requires less data and uses less computer time than the traditional Lidar backscatter glue method. For instance, in our case the HURL system glue coefficients determined using the LBM technique for a 24 h Lidar run can take ~3 h of computer run time to determine. Yet the data for the LMT are acquired in 15–30 min after warm up and glue coefficients are determined within 5 min or less. The reason that the LMT-determined glue coefficients are calculated so fast is that the LMT uses linear regression of the average AD and PC data for all "profiles" taken together, whereas the LBM performs regressions on each individual profile. Another advantage is that the glue coefficients may be obtained prior to a Lidar data run using the LMT, which would permit real-time Lidar images to use up-to-date glue coefficients as data are being acquired.

Much of this research was conducted at the Howard University Beltsville Campus during the graduate studies of the senior author in the department of Physics of Howard University. This research is currently supported by the NASA Post-Doctoral Program at Goddard Space Flight Center as administered by Oak Ridge Associated Universities through a contract with NASA. This research is also supported by the NASA Atmospheric Composition program managed by Ken Jucks. We would like to thank Bernd Mielke of Licel for helpful suggestions during the development of this manuscript.

References

1. D. D. Venable, D. N. Whiteman, M. Calhoun, A. O. Dirisu, R. Connell, and E. Landulfo, "A lamp mapping technique for independent determination of the water vapor mixing ratio calibration factor for a Raman lidar system," Appl. Opt. **50**, 4622–4632 (2011).
2. D. N. Whiteman, B. Demoz, P. Girolamo, J. Comer, I. Veselovskii, K. Evans, Z. Wang, M. Cadirola, K. Rush, G. Schwemmer, B. Gentry, S. H. Melfi, B. Mielke, D. Venable, and T. Van Hove, "Raman lidar measurements during the international H_2O project. Part I: instrumentation and analysis techniques," J. Atmos. Ocean. Technol. **23**, 157–169 (2006).
3. R. K. Newsom, D. D. Turner, B. Mielke, M. Clayton, R. Ferrare, and C. Sivaraman, "Simultaneous analog and PC detection for Raman lidar," Appl. Opt. **48**, 3903–3914 (2009).
4. D. Venable, E. Joseph, D. N. Whiteman, B. Demoz, R. Connell, and S. Walford, "Development of the Howard University Raman lidar," in *Second Symposium on Laser Atmospheric Applications held at the 85th Annual Meeting of the American Meteorological Society*, San Diego, California, 2005, http://ams.confex.com/ams/pdfpapers/85650.pdf.
5. M. Adam, D. Venable, R. Connell, E. Joseph, D. N. Whiteman, and B. B. Demoz, "Performance of the Howard University Raman lidar during 2006 WAVES campaign," J. Optoelectron. Adv. Mater. **9**, 3522–3528 (2007).
6. "Licel GmbH," Berlin, Germany, http://www.licel.com/transient_overview.html.
7. D. N. Whiteman, K. Rush, S. Rabenhorst, W. Welch, M. Cadirola, G. McIntire, F. Russo, M. Adam, D. Venable, R. Connell, I. Veselovskii, R. Forno, B. Mielke, B. Stein, T. Leblanc, S. McDermid, and H. Vomel, "Airborne and ground-based measurements using a high-performance Raman lidar," J. Atmos. Ocean. Technol. **27**, 1781–1801 (2010).
8. D. N. Whiteman, K. C. Vermeesch, L. D. Oman, and E. C. Weatherhead, "The relative importance of random error and observation frequency in detecting trends in upper tropospheric water vapor," J. Geophys. Res. **116**, D21118 (2011).
9. D. N. Whiteman, M. Cadirola, D. Venable, M. Calhoun, L. Miloshevich, K. Vermeesch, L. Twigg, A. Dirisu, D. Hurst, E. Hall, A. Jordan, and H. Vomel, "Correction technique for Raman water vapor lidar signal-dependent bias and suitability for water vapor trend monitoring in the upper troposphere," Atmos. Meas. Tech. **5**, 2893–2916 (2012).
10. R. D. Evans, *The Atomic Nucleus*, (McGraw-Hill, 1955).
11. D. N. Whiteman, S. H. Melfi, and R. A. Ferrare, "Raman lidar system measurement of water vapor and aerosols in the Earth's atmosphere," Appl. Opt. **31**, 3068–3082 (1992).
12. D. P. Donovan, J. A. Whiteway, and A. I. Carswell, "Correction for nonlinear photon-counting effects in lidar systems," Appl. Opt. **32**, 6742–6753 (1993).
13. D. N. Whiteman, "Examination of the traditional Raman lidar technique. I. Evaluating the temperature-dependent lidar equations," Appl. Opt. **42**, 2571–2592 (2003).
14. M. Adam, B. B. Demoz, D. N. Whiteman, D. D. Venable, E. Joseph, A. Gambacorta, J. Wei, M. W. Shephard, L. M. Miloshevich, C. D. Barnet, R. L. Herman, J. Fitzgibbon, and R. Connell, "Water vapor measurements by Howard University Raman lidar during the WAVES 2006 campaign," Bull. Am. Meteorol. Soc. **27**, 42–60 (2010).